

## Structural and morphological characterization of synthetic chrysotile single crystals

G. Falini, E. Foresti, G. Lesci and N. Roveri\*

Department of Chemistry 'G. Ciamician', Alma Mater Studiorum University of Bologna, I-40126 Via Selmi, 2, Bologna, Italy. E-mail: roveri@ciam.unibo.it

Received (in Cambridge, UK) 10th April 2002, Accepted 28th May 2002

First published as an Advance Article on the web 13th June 2002

Stoichiometric chrysotile single crystals have been synthesized as a unique phase by hydrothermal reaction under controlled conditions; the synthesized monocrystals show a cylinder-in-cylinder morphology and can be used as a reference sample with definite chemical composition to investigate the factors responsible of the chrysotile cytotoxicities and carcinogenicities.

There is a continuing interest in the investigation on chrysotile because of the health hazards associated with asbestos, of which chrysotile accounts for approximately 95% of world production.<sup>1,2</sup> It yields fibrogenesis and carcinogenesis of the respiratory system not only owing to the needle-like nature of its fibres, but mainly because of its chemical and structural characteristics.<sup>3</sup>

Chrysotile,  $Mg_3Si_2O_5(OH)_4$ , is the predominant fibrous form of serpentine. The crystal morphologies of the serpentines include cylindrical rolls (chrysotile), planar structures (lizardite, amesite and many unnamed aluminium species) and corrugated structures (antigorite).<sup>4</sup>

Chrysotile is constituted of sheets of tetrahedral silica in a pseudo-hexagonal network joined to sheets of octahedral magnesium hydroxide. On one side, two out of every three hydroxy groups are replaced by apical oxygen of the tetrahedral silica. X-Ray diffraction<sup>5,6</sup> and high-resolution TEM<sup>7</sup> investigations have defined the structure of mineral chrysotile fibrils as consistent with layers curled concentrically or spirally, usually around the  $x$  axis (orthochrysotile) and seldom around the  $y$  axis (parachrysotile), into a tubular structure of about 22–27 nm in diameter.<sup>5,7</sup> About 10 layers, each one 0.73 nm thick, constitute the wall thickness of the cylindrical rolls. The rolls possess hollow cores with a diameter of about 7–8 nm because the layers energetically cannot withstand too tight a curvature.<sup>5,8</sup> The distribution of dimensions of the inner and outer diameters of mineral chrysotile fibrils varies considerably from sample to sample, presumably depending on the growth conditions in each locality where the mineral samples arise.<sup>7</sup> Many studies have shown that serpentinites commonly contain two or three serpentine minerals which are so finely intergrown that they may be considered to form hybrid, or mixed structures.<sup>9</sup>

The presence in mineral chrysotile of foreign elements, structural disorder and heterogeneity affect not only their growth patterns, morphology, structure, shape, stiffness, strength, fracture characteristics, dissolution mechanisms, kinetics and surface catalytic activity, but also the biological–mineral system interaction.<sup>10,11</sup> In fact samples of mineral chrysotile from different localities have quite different biological activities.

The toxicity and pathogenicity of chrysotile is almost certainly dependent on a combination of mechanical-dimensional and chemical properties of the fibres.<sup>12</sup> Thus the availability of a synthetic chrysotile, which can be used as a reference sample, is crucial to investigate the different factors responsible for disease generation.

Chrysotile has been synthesized by hydrothermal reactions using the  $MgO-SiO_2-H_2O$  system,<sup>13</sup>  $Si_2Mg_3O_7$  gel and by transformation of synthetic diopside  $Ca Mg[Si_2O_6]$ <sup>14</sup> or natural

olivine.<sup>15</sup> The chrysotile fibres obtained from these syntheses showed different morphologies such as cone-in cone, cylinder-in-cylinder and polygonal fibres.<sup>16</sup>

Synthetic chrysotile has been previously prepared mainly with the aim to study the genesis of the mineral in geological environments and the contamination by foreign elements. The intergrowths with other serpentines (lizardite and antigorite) has been more frequently invoked than hindered.

In this communication, we present the synthesis and the characterization of stoichiometric chrysotile single crystals prepared as a unique phase under controlled conditions.† The powder X-ray diffraction pattern of the product displayed the characteristic reflections of chrysotile, as a unique crystalline phase (Fig. 1(a)). The starting pH, the reaction time, the Si/Mg molar ratio and the temperature of the hydrothermal treatment strongly affect the mineral purity and its degree of crystallinity. We found that a chrysotile Si/Mg molar ratio of  $\leq 0.66$  induced the precipitation of a secondary phase, brucite. With a Si/Mg molar ratio higher than 0.70, under the same conditions of temperature, pressure, pH and time, the crystallization of talc was observed together with chrysotile.

The FTIR and the Raman spectra of the natural chrysotile minerals show a range of absorption frequencies associated with the same vibration, depending on the place where it is has been mined. Pure synthetic chrysotile displays in the FTIR spectrum

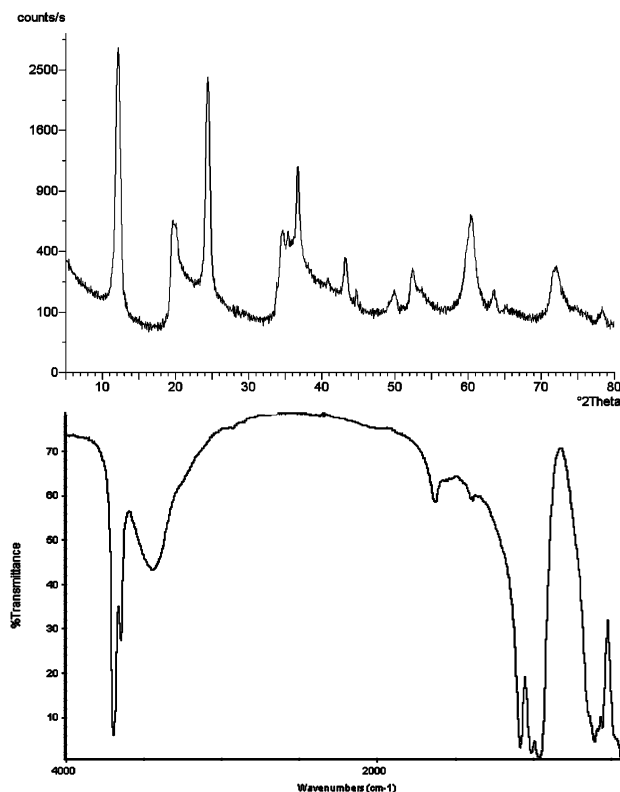
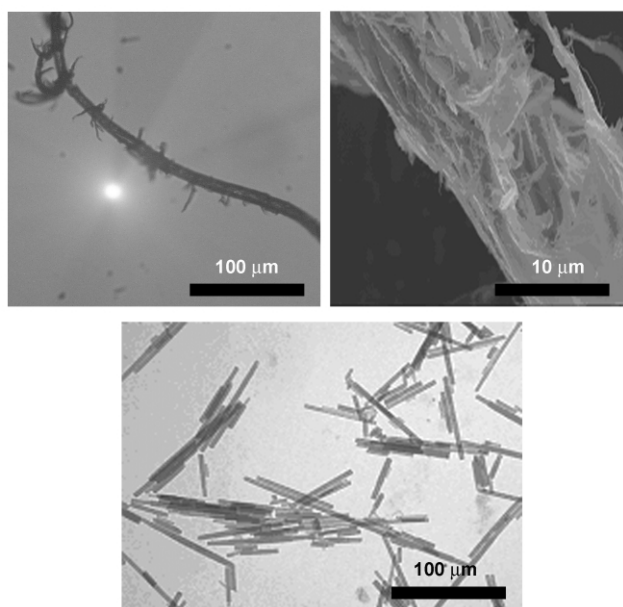


Fig. 1 Synthetic chrysotile: (a) X-ray diffraction pattern; (b) FTIR spectrum.

absorption bands at 3692 and 3645  $\text{cm}^{-1}$  due to OH stretching and at 1082 and 1015  $\text{cm}^{-1}$  due to Si–O stretching (Fig. 1(b)) and in the Raman spectrum at 3700 and 3685  $\text{cm}^{-1}$  due to OH stretching, at 1103, 689 and 623  $\text{cm}^{-1}$  due to Si–O–Si stretching and at 465, 432, 390, 346 and 233  $\text{cm}^{-1}$  due to Mg–O stretching. No absorption bands of appreciable intensity that could be attributed to any other chrysotile polymorphs or polytypes, have been observed.

Optical microscopy images of synthesized stoichiometric chrysotile display the presence of bundles with the typical chrysotile fibrous morphology and the presence of aggregates constituted of chrysotile nano-crystals (Fig. 2(a)). Scanning electron microscopy images show how the long bundles are constituted of finely matted fibres of very small size (Fig. 2(b)). The chrysotile aggregates were split by sonication and the sample analysed by transmission electron microscopy (TEM) without any additional treatment and Fig. 2(c) shows the observed chrysotile nano-crystals. They have a cylindrical morphology with a length of the order a micron. An electron diffraction pattern typical of a single crystal of chrysotile was obtained from each nano-crystal (data not shown). The single crystals showed a transparency in the central areas that run longitudinally along to the fibre axis (Fig. 3(a)). This indicates that the core of the crystals is void or contains low electron dense material, such as an amorphous phase. The cylinder-in-cylinder morphology is the only structure present (Fig. 3(a)). In



**Fig. 2** (a) Optical microscope image of a bundle of synthetic chrysotile. (b) Scanning electron microscopy image of the surface of a synthetic chrysotile bundle with some fibres being observable. (c) Transmission electron microscopy image of single chrysotile crystals.

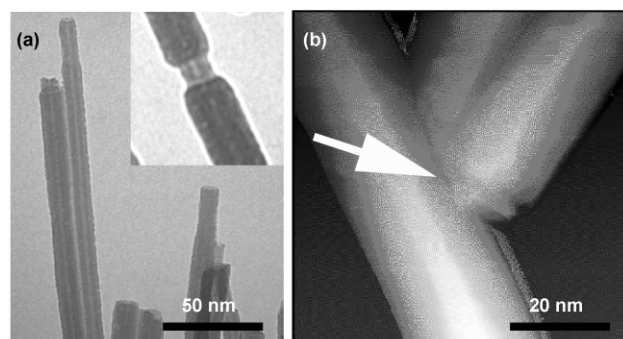


**Fig. 3** Transmission electron microscopy images (a) and atomic force microscopy image (b) of chrysotile single crystals. The cylinder-in-cylinder morphology is observable in the inset in (a). The arrow indicates the cylinder-in-cylinder morphology.

the mineral and in previously synthesized chrysotile<sup>16</sup> the cylinder-in-cylinder morphology is always associated with other morphologies such as cone-in-cone and the polygonal shapes, in addition to other multi-layer polytypes.

The observations by AFM of the synthesized single crystals not only evidence the cylinder-in-cylinder morphology (Fig. 3(b)), but also allowed to determine accurately their outer diameter ( $24 \pm 2$  nm) as well as the diameter of the inner cylinder ( $11 \pm 1$  nm). The wall thickness of the external tube is about 7 nm (AFM and TEM data). This observation indicates that about 10 layers are present, in agreement with the critical thickness for the mineral plane cleavage.

The petrogenetic relationship between the different serpentine structures is still unclear and is related to a partial substitution of Si and Mg by extraneous elements.<sup>17</sup> However this report indicates that chrysotile showing cylinder-in-cylinder morphology can be synthesized in the absence of extraneous elements. The introduction of extraneous elements, such as Al and Fe, and control over pH, thermal and kinetic parameters may be used to crystallize chrysotile fibres with different serpentine structures. This will open the possibility to investigate their crystal growth processes and their disease-generating interactions with biological systems.

Furthermore, a chrysotile is now available which can be used as a reference sample to investigate the chemical, physical and biological properties of the serpentines.

We thank Prof. A. Ripamonti for helpful discussion and criticism. This work was supported by MIUR, CNR and the University of Bologna (Funds for Selected Research Topics).

## Notes and references

† The synthetic method is a modification of that of Noll *et al.*,<sup>18</sup> using a Parr reactor 4564 with a 160  $\text{cm}^3$  vessel. The  $\text{SiO}_2$  mesophase MCM41<sup>19</sup> (kindly supplied by Prof. E. Caponetti, University of Palermo, Italy) was used as the starting material for the reactions in aqueous  $\text{MgCl}_2$  (Si/Mg molar ratio = 0.68). The pH of the gel mixture was raised to 13.0 by means of aqueous NaOH solution. The final volume of the mixture was 70  $\text{cm}^3$ , where the concentration of  $\text{MgCl}_2$  was 10 mM and NaOH 0.4 M. The hydrothermal treatment was carried out at 300 °C on the saturated vapour pressure curve (82 atm) with a reaction time of 24 h. The precipitate removed from the resulting solution was repeatedly washed with deionised water before being dried for 3 h at 150 °C.

- 1 M. Ross in *Amphiboles and Other Hydrous Pyriboles-Mineralogy, Reviews in Mineralogy*, ed. D. R. Veblen, Mineralogical Society of America, Washington, D.C., 1981, vol. 9A, p. 279.
- 2 H. Schreier, in *Asbestos in the Natural Environment*, Elsevier, New York, 1989, p. 159.
- 3 L. A. Hume and J. D. Rimstidt, *Am. Mineral.*, 1992, **77**, 1125.
- 4 B. T. Mossman, in *Health effects of mineral dust, Reviews in Mineralogy*, ed. G. D. Guthrie and B. T. Mossman, Mineralogical Society of America, Washington, D.C., 1992, vol. 28, p. 513.
- 5 E. J. W. Whittaker, *Acta Crystallogr.*, 1957, **10**, 149.
- 6 E. J. W. Whittaker, in *Mineralogical Techniques of Asbestos Determination*, ed. R. L. Ledoux, Mineral. Assoc., Canada, Montreal, 1979, p. 1.
- 7 K. Yada, *Acta Crystallogr., Sect. A*, 1971, **27**, 659.
- 8 B. A. Cressey and E. J. W. Whittaker, *Miner. Mag.*, 1993, **57**, 148.
- 9 D. R. Veblen and P. R. Buseck, *Science*, 1979, **206**, 1398.
- 10 M. Churg, B. Wiggs, L. Depaoli, B. Kampe and B. Stevens, *Am. Rev. Respir. Dis.*, 1984, **130**, 1042.
- 11 R. P. Nolan, A. M. Oechesle, G. W. Addison and J. Colflesh, in *Mechanisms in Fibre Carcinogenesis*, ed. R. C. Brown, Plenum Press, New York, 1991, p. 231.
- 12 B. Fubini and C. Otero Areàn, *Chem. Soc. Rev.*, 1999, **28**, 373.
- 13 J. V. Chernosky, Jr., R. G. Berman and L. T. Bryndzia, *Rev. Miner.*, 1988, **19**, 295.
- 14 E. Barrese, E. Belluso and F. Abbona, *Eur. J. Mineral.*, 1997, **9**, 83.
- 15 K. Yada and K. Iishi, *Am. Mineral.*, 1977, **62**, 958.
- 16 B. Devouard, A. Baronnet, G. Van Tendeloo and S. Amelinckx, *Eur. J. Mineral.*, 1997, **9**, 539.
- 17 J. V. Chernosky, *Am. Mineral.*, 1975, **60**, 200.
- 18 V. W. Noll, H. Kircher and W. Sybertz, *Kolloid-Z.*, 1958, 1.
- 19 C. T. Kresge, M. E. Leonowicz, W. J. Roth and J. Vartuli, *Nature*, 1992, **359**, 710.